

LIMITING PARAMETERS OF AN ARTIFICIAL CAVITY FORMED ON THE LOWER SURFACE OF A HORIZONTAL WALL

A. A. Butuzov

Mekhanika Zhidkosti i Gaza, Vol. 1, No. 2, pp. 167-170, 1966

The liquid weight has a significant effect on the detached cavitation flow which is artificially created by gas injection behind an obstacle (probe) in a liquid stream [1]. This paper considers two-dimensional cavitation flow created behind a projection on the lower surface of an infinite horizontal wall.

1. The problem of the cavitation flow about a plate which forms a small angle α with a wall is solved. The liquid is assumed to have weight and to be ideal and incompressible, and its motion is irrotational. The length L of the cavity is considerably greater than the length of the projection. The Ryabushinskii scheme is used.

Notation

- a — is the ratio of plate length to cavity half-length,
- $\eta(x)$ — is the ordinate of the cavity contour,
- f — is a quantity inverse to the square of the Froude number expressed in terms of the cavity half-length $L/2$,
- g — is the gravitational acceleration,
- U_0 — is the flow velocity at infinity,
- σ — is the cavitation number,
- p_0 — is the pressure at infinity at the level of the horizontal wall.
- p_k — is the pressure in the cavity,
- ρ — is the liquid density.

The problem consists of finding the complex induced flow velocity $w(z) = u(z) - iv(z)$, where u and v are the horizontal and vertical components of the induced velocity, $z = x + iy$. We use dimensionless values of the induced velocities and dimensionless coordinates. The induced velocities are referred to the magnitude of the undisturbed stream velocity at infinity, and the coordinates are referred to the cavity half-length.

The analytic function $w(z)$ must satisfy the condition of no fluid flow through the solid boundaries and the cavity contour and the condition of constant pressure on the cavity contour. In view of the thinness of the projection and consequently of the cavity as well, these boundary conditions are linearized. The boundary conditions have the form

$$v(x) = \omega(x) \quad (-\infty < x < \infty), \quad (1.1)$$

$$\omega(x) = -\alpha \quad (-1 - a < x < -1),$$

$$\omega(x) = -\eta'(x) \quad (-1 < x < 1),$$

$$\omega(x) = \alpha \quad (1 < x < 1 + a),$$

$$\omega(x) = 0 \quad (x < -1 - a, \quad x > 1 + a). \quad (1.2)$$

$$\text{Also, } u(x) = -f\eta(x) - 1/2\sigma \quad (-1 < x < 1), \quad (1.3)$$

where
$$\eta(x) = \alpha a + \int_{-1}^x v dx, \quad \int_{-1}^1 v dx = 0,$$

$$f = \frac{gL}{2U_0^2}, \quad \sigma = \frac{p_0 - p_k}{1/2\rho U_0^2}. \quad (1.4)$$

The cavity contour must be tangential to the projection contours, and therefore these conditions must be supplemented by the requirement

$$\eta'(-1) = -\eta'(1) = \alpha. \quad (1.5)$$

The function $w(z)$ may be represented by the integral relation

$$w = -\frac{1}{\pi} \int_{-1-a}^{1+a} \frac{\omega(\xi) d\xi}{\xi - z} \quad (1.6)$$

resulting from equalities (1.1), (1.2) and the Schwartz equation for the semiplane. Relations (1.2), (1.3), (1.6) lead to an integro-differential equation in terms of the function $\eta(x)$

$$f\eta(x) + \frac{1}{\pi} \int_{-1}^1 \frac{\eta'(\xi) d\xi}{\xi - x} + \frac{\sigma}{2} = \frac{\alpha}{\pi} \ln \frac{(1+a)^2 - x^2}{1-x^2}$$

for $-1 < x < 1$. (1.7)

At the points $x = \pm 1$ the function $\eta(x)$ must satisfy condition (1.5) and the condition

$$\eta(\pm 1) = \alpha a \quad (1.8)$$

resulting from equalities (1.4). The integro-differential Eq. (1.7) with conditions (1.5), (1.8) is equivalent to the boundary-value problem (1.1)-(1.5) for the analytic function $w(z)$. The parameter σ in (1.7), as in (1.3), is unknown.

The integro-differential equation (1.7) was solved approximately. To do this the function $\eta(x)$ at the intervals $\xi_i \leq x \leq \xi_{i+1}$, where the points ξ_m are chosen so that

$$-1 = \xi_{-n} < \xi_{-(n-1)} < \dots < \xi_{-1} < \xi_0 < \xi_1 < \dots < \xi_n = 1, \quad \xi_0 = 0, \quad \xi_{-m} = -\xi_m$$

was approximated by polynomials of second degree. The polynomials satisfied the conditions $\eta(\xi_i^+) = \eta(\xi_i^-)$, $\eta'(\xi_i^+) = \eta'(\xi_i^-)$, conditions (1.5), (1.8), and the condition $\eta(x) = \eta(-x)$ which results from the Ryabushinskii scheme.

This approximation for the function led to equalities of the form

$$\eta(x) = \eta(1) + \sum_{i=1}^n c_i(x) q_i. \quad (1.9)$$

$$\int_{-1}^1 \frac{\eta'(\xi) d\xi}{\xi - x} = \sum_{i=1}^n d_i(x) q_i \quad (0 < x < 1), \quad q_n = -\eta'(1) = \alpha.$$

Here q_i are the values of the function $\eta'(x)$ at the points $x = \xi_1, \xi_2, \dots, \xi_n$; the functions $c_i(x), d_i(x)$ depend on the selection of the points ξ_m . Equation (1.7) was satisfied at the points $x = 1/2(\xi_i + \xi_{i+1})$, $i = 0, 1, 2, \dots, n-1$. Thus, in accordance with equalities (1.9), a system of n linear algebraic equations with n unknowns was composed:

$$\sigma/\alpha, q_1/\alpha, \dots, q_{n-1}/\alpha.$$

The system of linear equations was solved on the M-20 electronic computer. In order to verify the convergence of the approximate solutions of the integro-differential equation, we considered the cases $n = 10$ and $n = 20$, and also the exact solution of Eq. (1.7) for $f = 0$ [2]. The calculations were made for four values of the parameter a : 0.2, 0.1, 0.05, 0.025, and values of the parameter f varying in the range $0 \leq f \leq 3.2$.

The results of the calculations were identical for all values of the parameter a . The variation of the quantity σ/α as a function of the parameter f for the case $a = 0.1$, as plotted from the computational results, is shown in Fig. 1b. The circles in the figure denote the points corresponding to the system of 20 equations; the crosses are for

the system of ten equations. The variation of the quantity g_i/α as a function of the parameter f is similar in nature: with increases of the parameter f the quantities q_i/α vary continuously at first, and then undergo a sudden change.

As shown by the calculations, the range of values of the parameter f in which the characteristics of the cavitation flow vary jump-wise does not depend on the value of the parameter α and is given by the inequality $2.60 < f < 2.88$. Outside of this range the convergence of the approximate solutions is satisfactory. Thus, outside of the interval $2.60 < f < 2.88$ the values of σ/α found from the systems of equations with ten and twenty unknowns differ from one another by less than 3-8%. For $f = 0$ the exact values of σ/α differ from the approximate values by less than 3%.

The discontinuous variation of the quantities q_i/α according to the computational data leads to the situation where the cavity contour $\eta(x)$ pierces the wall. Consequently, the cavity cannot exist in some range of large values of the parameter f . The range of small values of the parameter f in which the cavity can exist is bounded above by the limiting value f_* ($2.60 < f_* < 2.88$). The value f_* of the parameter corresponds to the limiting value of the Froude number in terms of the cavity length $F_* = 1 / \sqrt{2f_*}$ ($0.416 < F_* < 0.438$), and for $U_0 = \text{const}$ it is the limiting cavity length L_* . In the case of continuous increase of the cavity length for a fixed stream velocity U_0 , there cannot be a cavity with a length exceeding the limiting value.

The discontinuous variation of the parameters of the cavitation flow indicates the passage through zero of the determinant of the system of algebraic equations which replace the integro-differential equation. From this it may be shown that the limiting Froude number corresponds to the condition which admits the existence on a smooth wall of thin cavities whose contour approaches the wall asymptotically at the forward and rear points. Actually, such cavities are described by relations (1.7), (1.5), (1.8) for $\alpha = 0$. In the case $\alpha = 0$ the corresponding system of linear algebraic equations in terms of the unknowns σ, q_i , according to equalities (1.9), is homogeneous. The system has a nontrivial solution only for a zero value of its determinant, i. e., under the condition $f = f_*n$, where $f_*n \rightarrow f_*$ as $n \rightarrow \infty$, n being the number of equations in the system.

2. The conclusions drawn above are valid for thin cavities. The assumption of thinness of the cavity may be realized theoretically for values of the parameter F ($F > F_*$), infinitely close to the limiting value, since the quantity α may be selected sufficiently small. However, if we fix the angle α , unlimited increase of the relative thickness of the cavity (ratio of the cavity thickness to its length) with the reduction of the Froude number which is predicted by the linear theory leads to the situation where the linear theory becomes invalid before the value $F = F_*$ is reached. Since the limitation $F > F_*$ is of primary interest, we present below an approximate analysis of the cavitation flow which is free from any assumption as to cavity thinness. The analysis is based on the assumption that the linear theory qualitatively reflects correctly the nature of the relationship between the cavitation flow parameters for $F > F_*$.

Let us assume that for some fixed value of F ($F > F_*$) a thin cavity is obtained behind the projection probe. If we gradually increase the pressure in the cavity, without varying the stream velocity U_0 , according to the assumption made above the cavity length will increase. After some value of the parameter σ is reached, the relative thickness of the cavity will also increase. When the relative cavity thickness becomes sufficiently large, the projection practically ceases to play any part in the formation of the cavity. The contour of the cavity which exists without the projection may either be tangential to the wall or may form some angle with it. The first case was considered qualitatively in the preceding section of this paper. Let us turn to the second case. In this, the point of the cavity contour which lies on the wall will be a stagnation point and therefore, according to the Bernoulli equation, the following conditions must be satisfied:

$$\sigma = -1, \quad \left(\frac{W}{U_0}\right)^2 = \frac{2\kappa}{U_0^2} \eta(x) \quad (2.1)$$

Here W is the velocity on the cavity contour and $\eta(x)$ is the dimensional ordinate of the cavity contour. The question on the existence of a cavity whose shape satisfies (2.1) is equivalent to that on the existence of a body which is symmetrical with respect to the horizontal axis, with the velocity distribution law along its surface

$$\left(\frac{W}{U_0}\right)^2 = k \frac{\eta(x)}{c} \quad (2.2)$$

Here k is a dimensionless constant and c is a characteristic linear dimension of the body.

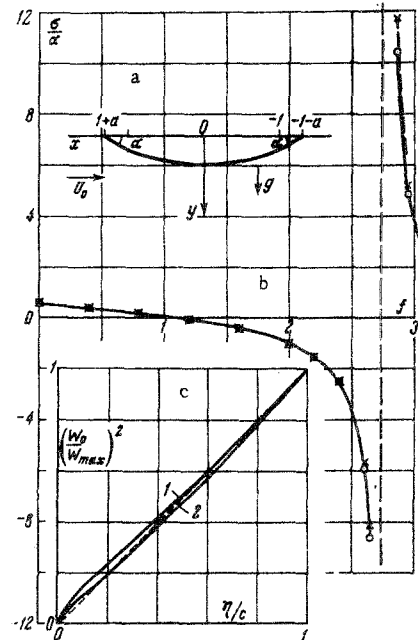


Fig. 1

If a body of such a shape exists, then the linear dimensions of the cavity are defined by the equality

$$c = k \frac{U_0^2}{2g} \quad (2.3)$$

Considering bodies of differing shape, it was found that a lune with a 90° angle at the vertex comes very close to satisfying condition (2.2). For example, in Fig. 1c the solid lines 1 and 2 show the dependence of $(W/W_{max})^2$ on η/c ($c = \eta_{max}$) for lunes with vertex angles of $2\beta = 90^\circ$ and $2\beta = 100^\circ$. The broken curve corresponds to the desired relation, transformed to the form

$$(W / W_{max})^2 = \eta / c, \quad (c = \eta_{max}) \quad (2.4)$$

The cavity parameters which satisfy conditions (2.1) may be defined approximately on the basis of the approximation of its contour by a circular arc which approaches the wall at the angle $\beta = 45^\circ$. In this case it is convenient to use the relation

$$k = \left(\frac{W_{max}}{U_0}\right)^2 \quad (2.5)$$

resulting from equality (2.2). The relative thickness of the cavity and the Froude number thus obtained, respectively, have the values

$$\delta = \eta_{max} / L = 0.207, \quad F = U_0 / \sqrt{gL} = 0.423 \quad (2.6)$$

This Froude number is in agreement with the limiting Froude number obtained from the linear theory.

This analysis permits the following conclusion to be drawn. Increase of the pressure ($U_0 = \text{const}$) in a thin long cavity leads to the formation of a cavity independent of the projection — a free cavity. The free cavity has maximal length and may have one of two types of contour: either tangential to the wall or approaching it at some angle. The second type of cavity, since it corresponds to the minimal

possible cavitation number $\sigma = -1$, is the limiting case of the first type. The free cavity is not formed by the probe and therefore may separate from it, being located in any region of the horizontal wall. As the limiting parameters of the cavity formed behind a projection we can take the parameters of the free cavity: $F_* \approx 0.423$, $\delta_* \approx 0.207$, and $\sigma_* = -1$.

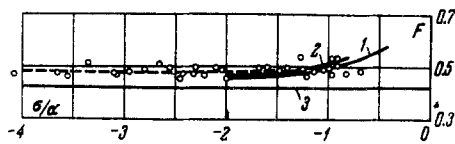


Fig. 2

3. An experiment was conducted in a water tunnel to verify the theoretical results obtained. The test specimen was a flat plate with side plates, with air being supplied to the bottom surface. The plate length was 945 mm, width 200 mm, thickness 20 mm, the distance from the leading edge of the plate to the probe was 315 mm, and the distance between the bottom of the plate and the lower edge of the side plate was 295 mm. The plate was immersed to 120 mm. The experiments were conducted with a wedge-shaped projection having a length of 12 mm and height of 2 mm. The test was run with stream velocities up to 0.7 m/sec. The air was supplied to the cavity through an opening in the plate, shielded by an anti-entrainment device; the opening had a diameter of 10 mm and was located at a distance of 70 mm behind the projection. The cavity was first formed by pumping air through a slot directly behind the projection. Stream velocity, air flow rate, cavity pressure, and cavity parameters were measured in the course of the tests.

The experimental data showed that with an increase of the air flow rate the cavitation number diminished and the cavity dimensions increased. In the final analysis increase of the cavity dimensions led to a separation of the cavity from the projection. On leaving the projection, the cavity in all cases moved upstream, after which it occupied a position such that the opening of the tube which supplied the air was located at the end of the cavity. The leading section of the cavity surface which had left the wedge had a regular form and always approached the plate at a considerable angle; the

trailing section was strongly distorted by the turbulent air stream leaving the cavity.

The results from the measurements of the cavity length are shown in Fig. 2. Here the values of the Froude number $F = U_0 / \sqrt{gL}$ are plotted along the vertical axis, and the ratios of the cavitation number to the wedge aperture angle σ/α ($\alpha = 1/6$) are plotted along the horizontal axis. The experimental points denoted by circles cover the range of variation of the parameter $f_1 = af$ from 0.21 to 0.31. The broken curve is experimental, while the solid curves 1 and 2 correspond to calculation using the linear theory, for $f_1 = 0.21$ (curve 1) and for $f_1 = 0.31$ (curve 2). The horizontal line 3 corresponds to the limiting Froude number $F_* = 0.423$. The points lying in the right side of the figure are for the thin cavities; the points farthest to the left ($\sigma < -0.5$) correspond to the cavities observed just prior to separation from the wedge, i.e., limiting cavities. According to these experiments, the limiting parameters F_* and δ_* for the cavities are $F_* \approx 0.48$, $\delta_* \approx 0.14-0.17$; the limiting cavitation number $\sigma_* \approx -(0.5-0.6)$.

Comparison of the limiting cavity parameters obtained theoretically and experimentally indicates that in reality the flow critical region, i.e., the separation of the cavity from the wedge, is observed earlier than theory predicts — for larger values of the cavitation number. This may be explained by the effect of liquid viscosity. Actually, the cavities having the greatest thickness must create a considerable pressure gradient along the plate, which may lead to separation of the boundary layer and, thus, to a reduction of the pressure at the presumed critical point. This pressure reduction is equivalent to an increase of the limiting cavitation number.

In summary the data from these experiments indicate satisfactory qualitative agreement between theory and experiment.

REFERENCES

1. A. D. Pernik, Cavitation Problems [in Russian], Sudpromgiz, 1963.
2. N. I. Muskhelishvili, Singular Integral Equations [in Russian], Gostekhizdat, 1946.

16 April 1965

Leningrad